

AD-A191 150

BEST  
AVAILABLE COPY

DTIC FILE COPY

## Application of Chaos Theory to $1/f$ Noise

Prepared by

A. FCTE, S. KOHN, and E. FLETCHER  
Chemistry and Physics Laboratory  
Laboratory Operations  
and  
J. McDONOUGH  
Vehicle and Control Systems Division  
Engineering Group  
The Aerospace Corporation  
El Segundo, CA 90245

12 February 1988

Prepared for

SPACE DIVISION  
AIR FORCE SYSTEMS COMMAND  
Los Angeles Air Force Base  
P.O. Box 92960, Worldway Postal Center  
Los Angeles, CA 90009-2960

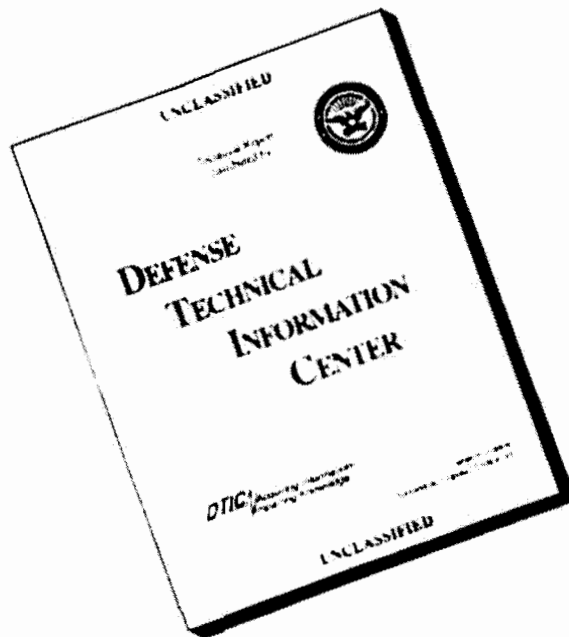
APPROVED FOR PUBLIC RELEASE;  
DISTRIBUTION UNLIMITED

DTIC  
ELECTE  
MAR 11 1988  
S H D

88 8 0

200

# DISCLAIMER NOTICE



THIS REPORT IS INCOMPLETE BUT IS THE BEST AVAILABLE COPY FURNISHED TO THE CENTER. THERE ARE MULTIPLE MISSING PAGES. ALL ATTEMPTS TO DATE TO OBTAIN THE MISSING PAGES HAVE BEEN UNSUCCESSFUL.

UNCLASSIFIED

SECURITY CLASSIFICATION OF THIS PAGE

## REPORT DOCUMENTATION PAGE

1a. REPORT SECURITY CLASSIFICATION Unclassified			1b. RESTRICTIVE MARKING AD-497130	
2a. SECURITY CLASSIFICATION AUTHORITY			3. DISTRIBUTION/AVAILABILITY OF REPORT Approved for public release; distribution unlimited.	
2b. DECLASSIFICATION/DOWNGRADING SCHEDULE				
4. PERFORMING ORGANIZATION REPORT NUMBER(S) TR-0086A(2945-07)-2			5. MONITORING ORGANIZATION REPORT NUMBER(S) SD-TR-88-29	
6a. NAME OF PERFORMING ORGANIZATION The Aerospace Corporation Laboratory Operations		6b. OFFICE SYMBOL (If applicable)		7a. NAME OF MONITORING ORGANIZATION Space Division
6c. ADDRESS (City, State, and ZIP Code) El Segundo, CA 90245			7b. ADDRESS (City, State, and ZIP Code) Los Angeles Air Force Base Los Angeles, CA 90009-2960	
8a. NAME OF FUNDING/SPONSORING ORGANIZATION		8b. OFFICE SYMBOL (If applicable)		9. PROCUREMENT INSTRUMENT IDENTIFICATION NUMBER F04701-85-C-0086
8c. ADDRESS (City, State, and ZIP Code)			10. SOURCE OF FUNDING NUMBERS	
			PROGRAM ELEMENT NO.	PROJECT NO.
			TASK NO.	WORK UNIT ACCESSION NO.
11. TITLE (Include Security Classification) Application of Chaos Theory to 1/f Noise				
12. PERSONAL AUTHOR(S) A. Fote, J. McDonough, S. Kohn and E. Fletcher				
13a. TYPE OF REPORT		13b. TIME COVERED FROM _____ TO _____		14. DATE OF REPORT (Year, Month, Day) 1988, Feb 12
				15. PAGE COUNT 46
16. SUPPLEMENTARY NOTATION				
17. COSATI CODES			18. SUBJECT TERMS (Continue on reverse if necessary and identify by block number)	
FIELD	GROUP	SUB-GROUP		
			Photodiodes; Mercury Cadmium Telluride	
19. ABSTRACT (Continue on reverse if necessary and identify by block number)				
<p>1/f noise limits the sensitivity of HgCdTe photodiodes operated in the low frequency "staring" mode. Because other theories have failed to account for 1/f noise as a general phenomenon, the applicability of chaos theory in this material is investigated. 1/f noise data from HgCdTe photodiodes are applied to the analytic technique of R. Grassberger and I. Procaccia. Analysis indicates that a chaotic phenomenon underlies the 1/f noise. Construction of a model of 1/f noise in HgCdTe photodiodes consistent with the principle of chaos theory and the body of experimental knowledge about this phenomenon is begun. Initial model produced a 1/f<sup>a</sup> noise spectrum with a having a value close to 2.</p>				
20. DISTRIBUTION/AVAILABILITY OF ABSTRACT <input checked="" type="checkbox"/> UNCLASSIFIED/UNLIMITED <input type="checkbox"/> SAME AS RPT <input type="checkbox"/> DTIC USERS			21. ABSTRACT SECURITY CLASSIFICATION Unclassified	
22a. NAME OF RESPONSIBLE INDIVIDUAL			22b. TELEPHONE (Include Area Code)	22c. OFFICE SYMBOL

# CONTENTS

I.	INTRODUCTION.....	3
II.	HgCdTe PHOTODETECTORS.....	5
III.	MODELS OF 1/f NOISE.....	7
IV.	CHAOS THEORY.....	11
V.	ANALYSIS OF DATA.....	15
VI.	ANALYSIS OF HgCdTe PHOTODIODE DATA.....	17
VII.	CHAOTIC MODELING OF 1/f NOISE.....	21
VIII.	SUMMARY.....	23
	REFERENCES.....	25
	FIGURES.....	27
	APPENDIX.....	45



Accession For	
NTIS GRA&I	<input checked="" type="checkbox"/>
DTIC TAB	<input type="checkbox"/>
Unannounced	<input type="checkbox"/>
Justification	
By	
Distribution/	
Availability Codes	
Dist	Avail and/or Special
A-1	

## I. INTRODUCTION

The type of noise known as " $1/f$ " noise is a universal phenomenon, found in measurements as diverse as of the Earth's rotation, seasonal temperature variations, the neutron flux in the terrestrial magnetosphere, the flow of sand in an hourglass, the frequency of sunspots, the light output of quasars, the flow rate of the Nile, and the parameters of electronic devices. In spite of its widespread occurrence in such diverse and often simple systems,  $1/f$  noise has defied explanation by conventional theories.<sup>1-5</sup>

In electronic devices,  $1/f$  noise appears whenever current is carried by a small number of carriers or is forced to pass through a bottleneck. Such bottlenecks include very thin films, surface conducting layers, potential barriers at contacts, and the points of contact between individual grains in granular conductors. It usually has a very slight temperature dependence and is proportional to the current squared. In addition to an applied voltage, it can be induced by a temperature gradient.

As a particular example of electronic devices,  $1/f$  noise limits the sensitivity of HgCdTe infrared detectors operated in the low frequency "staring mode", the preferred mode for high spatial and temporal resolution observations. This research concentrates upon  $1/f$  noise measured in such HgCdTe devices.

$1/f$  noise obtains its name from its power spectral density, which varies with the inverse of the frequency (Fig. 1). Thus, in electronic applications, the lower the frequency at which one wishes to operate, the more troublesome this source of noise becomes. No lower frequency limit to the  $1/f$  spectrum has been found, even with measurements down to  $5E-7$  Hz. This remains inexplicable because the lack of a low frequency rollover would result in the dissipation of an infinite amount of energy in the noise. The noise extends to very high frequencies as well. It has been measured in carbon resistors at  $1E+6$  Hz.<sup>1-5</sup>

In electronic devices, it is established that  $1/f$  noise results from fluctuations in resistance. This conclusion emerges from the fact that  $1/f$  noise appears only in the presence of a current. However, in a novel measurement, Voss and Clarke found an even better way to demonstrate this connection. They measured the fluctuations in the magnitude of the Johnson

noise in samples of niobium, InSb, and carbon paper resistors and found that these fluctuations had a  $1/f$  spectrum. Since Johnson noise is proportional to resistance only, the  $1/f$  type of fluctuations in the Johnson noise indicated that the resistances of these materials also fluctuated in this manner and were, in fact, the origin of the  $1/f$  noise.

This result still leaves the question of whether the carrier density or the mobility causes the resistance of a sample to fluctuate. Another type of measurement has apparently settled this issue. By measuring the noise in the thermoelectric voltage of intrinsic and extrinsic semiconductors, and performing some rather lengthy analyses, some researchers have concluded that it is the mobility that fluctuates to produce  $1/f$  noise.<sup>3</sup> We will soon present further evidence that mobility fluctuations lie at the heart of  $1/f$  noise.

A major division of opinion exists as to whether  $1/f$  noise originates in the bulk or at the surface of a material. Much data can be cited to support either contention. It is well known, for example, that the type of surface etching employed in sample preparation will affect the magnitude of  $1/f$  noise. Also, for germanium single crystals, the composition of the ambient atmosphere affects the magnitude of the  $1/f$  noise by 10-20 dB. In the specific case of HgCdTe photoconductors and photodiodes, researchers have demonstrated that the magnitude of the  $1/f$  noise could be increased upon the application of a voltage at the material's surface. These examples seem to provide strong evidence for the surface origin of  $1/f$  noise.<sup>1</sup> On the other hand, it appears possible that  $1/f$  noise remains, even with the best of all conceivable surface preparation techniques, and that this residual noise is a fundamental property of the bulk material.

## II. HgCdTe PHOTODETECTORS

The research on  $1/f$  noise in HgCdTe photodetectors has duplicated many of the controversies of the field in general. For example, fervent advocates of both the surface and the bulk theories exist.<sup>6-8</sup> However, in one particular case, considerable agreement occurs. Most believe that, in HgCdTe at least, the phenomenon of  $1/f$  noise is strongly related to, and probably arises from, generation-recombination processes such as those that produce leakage currents in p-n junction diodes.

A variety of leakage current mechanisms act to limit the resistance of p-n junction diodes. At higher temperatures, the leakage arises predominantly from diffusion currents. Specifically, electrons and holes diffuse across the junction because of the existence of the large carrier concentration gradient there. At lower temperatures, this "diffusion current" falls below another leakage current, the generation-recombination or g-r current, which then becomes dominant. This current arises from the spontaneous creation and annihilation of mobile electron-hole pairs in the junction region. Both the diffusion current and the g-r current generate their own type of noise. Thus, we speak of the g-r noise as that arising from the g-r leakage current.

A number of experiments have demonstrated a clear correlation between the magnitude of the g-r current or noise and the magnitude of the  $1/f$  noise in HgCdTe photodetectors.<sup>6-8</sup> One particular study showed that the  $1/f$  noise was proportional to the g-r current for 14 variable area diodes (Fig. 2).<sup>7</sup> Meanwhile, the  $1/f$  noise does not increase with the photo-induced current, which is essentially a diffusion current. Thus, only the g-r current, not the total current, contributes to  $1/f$  noise in HgCdTe photodiodes.

Since the  $1/f$  noise did not increase with the diffusion current, and the noise was found to be independent of the p-side thickness, the study by Bajaj et al.<sup>8</sup> ruled out the bulk n- and p-regions as ultimate sources. Since they discounted the surface as well, they settled upon the depletion region as the origin of the  $1/f$  noise. Further support for this conclusion comes from the observation that the  $1/f$  noise depends strongly on applied voltage and most of the voltage drop is across the depletion region.

### III. MODELS OF 1/f NOISE

Attempts to account for 1/f noise using conventional approaches have failed because of the unusual features of this type of noise. The small temperature dependence presents one major difficulty. It apparently rules out thermally driven processes, such as those that drive Johnson and other noise currents, as responsible for the 1/f fluctuations.

The enormous frequency range of the 1/f spectrum has created another severe stumbling block to conventional theories of its origin. For example, suppose we speculate that 1/f noise is due to free electrons becoming temporarily bound to impurity atoms or defects, thereby remaining immobile for some average length of time. With many electrons falling in and out of such "traps", the overall free electron concentration would fluctuate and produce similar fluctuations in the resistance. Alternatively, we might suppose that upon becoming bound to such traps, the electrons could alter the scattering mechanisms of the lattice and hence cause the resistance fluctuations because of the resultant mobility fluctuations.

In such cases, the resultant noise spectrum would display a time constant indicative of the average time of occupancy of the traps. In order to achieve the very wide frequency range exhibited by 1/f noise, our model must include a superposition of processes with an equally wide range of time constants. In particular, any model of 1/f noise based upon trapping requires a distribution of time constants,  $\tau$ , with a weight,  $g(\tau)$ , described by

$$g(\tau) = A/(\tau)^2$$

Inventing a theory that produces this distribution of time constants has proven as troublesome as explaining the 1/f noise spectrum directly.

A general theory due to McWhorter deals with the time constant problem by having electrons enter and leave the traps at the material's surface by means of the quantum mechanical process of tunneling. Specifically, they tunnel through some potential energy barrier at the surface, such as could be caused by an oxide layer.



One strength of the McWhorter model is that the tunneling mechanism has a weak temperature dependence, as does  $1/f$  noise. Also, the probability that an electron can penetrate a barrier by tunneling varies exponentially with the thickness of the barrier. As a result, a barrier which varies slightly in thickness over the surface would produce a very wide distribution of time constants, such as is required. Nevertheless, the theory has deficiencies. The time constant distribution does not automatically acquire the proper weighting. In addition, experimental data do not fully support the McWhorter theory. It turns out that practically any surface treatment affects the magnitude of  $1/f$  noise but not its spectrum. From the theory, we would have expected that the addition or removal of surface layers would affect the distribution of time constants and, as a result, the spectrum of the noise.<sup>4</sup>

A bulk theory of  $1/f$  noise has long been advocated by Vandamme, Hooge, and Kleinpenning. Their belief hinges upon the discovery of an empirical relation that seems to exist between the  $1/f$  power spectral density,  $S_V$ , and the total number,  $N$ , of free carriers in the sample.<sup>3</sup> The relation is

$$S_V/V^2 = \alpha df/Nf$$

where  $df$  is the bandwidth of the measurement apparatus,  $f$  is the frequency, and  $\alpha$  is a universal constant with a magnitude of approximately  $2E-3$ . This relation has been shown to hold for a wide range of metals, and both  $n$ - and  $p$ -type semiconductors. The fact that  $N$  is the total number of carriers in the sample indicates a bulk effect (Fig. 3).<sup>3,9</sup>

However, the difficulties with this model are several. First, " $\alpha$ " does not appear to be that good of a universal constant. For silicon diodes, fits to the data require values for " $\alpha$ " of  $6E-3$  and  $1E-4$ , a large variation from the supposedly fundamental value of  $2E-3$ .<sup>10</sup>

Second, the model is more of an empirical correlation between parameters than a working theory of  $1/f$  noise. It merely postulates some unknown mechanism for producing mobility fluctuations. Thus, it does not tell us whether the noise can ultimately be eliminated. Finally, in the case of HgCdTe  $p$ - $n$  junctions, mobility fluctuations cannot explain why the  $1/f$  noise is seen in the leakage current due to generation-recombination but not in the leakage current due to diffusion.

Numerous other theories of  $1/f$  noise have appeared, and all of them suffer deficiencies of one sort or another.<sup>1-5</sup>

#### IV. CHAOS THEORY

All of the standard theories of noise,  $1/f$  or otherwise, have one major feature in common. They all attribute noise to some sort of random process, and in many cases that random process is thermally driven. However, we know that erratic looking behavior need not have a random driver. Consider the case of turbulent flow of a fluid. When flow velocities exceed critical values, the placid laminar flow will break up into a complex and unpredictable pattern of swirls and eddies, and this transition to turbulence occurs without the assistance of any random process. The equations that describe hydrodynamic systems, the Navier-Stokes equations, are entirely deterministic. When erratic behavior arises from deterministic equations, we now refer to it as "chaotic" in order to distinguish it from that driven by random processes.

Up until very recently, we lacked the mathematical sophistication to analyze chaotic behavior. However, that situation is changing rapidly. We are now beginning to understand the conditions that lead to chaos. For example, although the Navier-Stokes equations that give rise to turbulence in fluids are exceedingly complex, we now know that chaotic behavior can result from surprisingly simple equations. All that one requires is some sort of dissipative process along with nonlinear coupling between dependent variables.

Linked with the notion of chaos is a mathematical construct known as a "strange attractor".<sup>11</sup> To understand the concept of an attractor, see Fig. 4. Suppose we have a system describable by the phase space variables  $x_1$  and  $x_2$ . A pendulum, for example, will have phase space coordinates for position,  $x$ , and momentum,  $p$ . Suppose, further, that the system engages in some type of orderly periodic motion. In this case, the trajectory representing the evolution of the system in phase space will repetitiously retrace the same simple path. In the case of our pendulum, phase space will be represented by a two-dimensional graph with axes for  $x$  and  $p$ , and the trajectory will be an ellipse. Furthermore, if the system does not initially follow this ellipse, it will eventually evolve to do so. The phase space trajectory is "attracted" to this ellipse as the stable solution for the motion. Thus, we refer to the ellipse as an "attractor". In contrast, a randomly driven system would be represented by a phase space trajectory that wanders erratically over the entire graph.

Most systems of interest involve more than two phase-space parameters. In these cases, the attractor is a curve winding through a multidimensional phase space. To visualize an attractor in such cases, we look at a two-dimensional slice of the complete phase space and construct a "Poincaré once-return map". Where the trajectory passes through the Poincaré section, we mark a dot, something like a hole left by a moving bullet. With each subsequent pass, another dot appears. If our system is describable by a periodic behavior, the sequence of dots will "walk" towards a single dot, the attractor, and remain there forevermore. For random behavior, on the other hand, the dot pattern would resemble a shotgun blast.

Also shown in the figure is the case of a quasi-periodic attractor. Instead of a single dot, our bullet may repetitiously pass through a well defined set of dots forming a (possibly quite complicated) limit cycle.

Finally, we come to the case of a "strange attractor", also shown in Fig. 4. Our set of dots does not converge to a single dot or to a small set of dots. On the other hand, they are not random either. Instead, the dots converge onto an extremely complex pattern of dots. This pattern is the "strange attractor," and its existence marks the presence of chaotic behavior.

A strange attractor and the resultant chaotic behavior can arise from very simple equations. An example is the Henon attractor shown in Fig. 5. It results from the following equations between the two parameters  $x_1$  and  $x_2$ ,

$$x_1 = 1 + x_2 - ax_1^2$$

$$x_2 = bx_1$$

with  $a = 1.4$  and  $b = 0.3$ . To construct the attractor, we plot each  $(x_1, x_2)$  pair and then use the above equations to calculate the next pair. When we do so, we find that the plotted points appear seemingly at random on the graph, but nevertheless produce a clearly recognizable pattern. And, were we to simply plot one of the parameters vs time, as is done in Fig. 6, we see that we would be hard pressed to distinguish the result from a plot of random noise.

Of particular interest in chaos theory is the transition into a chaotic state. Fluid systems, for example, often evolve from laminar to turbulent flow

as the Reynolds number,  $R_e$ , is increased above some critical value. We can observe this transition in the mathematics by watching the behavior of the attractor. At low  $R_e$ , the system is typified by a normal attractor. But, when  $R_e$  exceeds a critical value, that attractor loses its stability and is replaced by a qualitatively different attractor, as indicated schematically in Fig. 7. Mathematically this process is termed a bifurcation. Further increases in Reynolds number may lead to additional bifurcations; it was shown by Ruelle and Takens<sup>12</sup> that only three or four such transitions are required to reach a chaotic state in the equations of fluid motion.

Figure 8 shows how the power spectrum evolves with the bifurcations. The upper curve displays the power spectrum of a periodic signal typified by a normal attractor. It exhibits a fundamental frequency and a few harmonics. The lower curve shows a spectrum after four period-doubling bifurcations. The system appears to be halfway in evolution between a set of discrete frequencies and a  $1/f$  type of spectrum. It is this type of result that first led us to believe that the answer to the enigma of  $1/f$  noise lay in chaos theory.

## V. ANALYSIS OF DATA

As previously mentioned, all existing theories of  $1/f$  noise have incorporated random processes. If, on the other hand,  $1/f$  noise has a chaotic nature, these theories cannot be valid. It is of interest, therefore, to determine whether  $1/f$  noise is random or chaotic. In the last few years, theorists have been attempting to develop methods whereby experimental noise data can be analyzed as to its random or chaotic nature.

Currently, one of the best available techniques to distinguish random from chaotic behavior is that developed by P. Grassberger and I. Procaccia.<sup>13</sup> The basis of the approach is to construct the attractor from the data and then determine its dimensionality. If we again study the case of the Henon attractor in Fig. 5, we note that it is a "fractal"; that is, it is an object with a noninteger dimensionality. As we examine it to greater detail, we find ever deeper layers of structure, showing that it is not merely a simple one-dimensional curve. On the other hand, since it does not fill the two-dimensional space of our plot, it is not two dimensional either. It has a dimensionality between 1 and 2. In contrast, purely random data would fill the space and have a dimensionality of 2.

We call the dimensionality of the attractor its fractal dimension and the dimensionality of the graph the "embedding" dimension. Chaotic behavior is typified by a fractal dimension which is noninteger and less than the embedding dimension. Random behavior has a fractal dimension which equals the embedding dimension. Thus, in order to distinguish chaotic from random behavior, we need merely construct the attractor and check its dimensionality as a function of the embedding dimension.

The Grassberger-Procaccia algorithm allows us to determine the dimensionality of an attractor mathematically. The justification of the procedure is lengthy and will not be gone into here. One begins with a set of  $N$  noise measurements,  $X_n$ , separated by a fixed time interval. From these data, one calculates a correlation function,  $C_d(r)$ , which is  $N^{-2}$  times the number of data pairs  $(m,n)$  for which the distance between phase space points is less than  $r$ .

$$C_d(r) = \left\{ \sum_{m,n=1}^N H[r - ||x_m - x_n||] \right\} / N^2$$

where  $H$  is the Heaviside function and  $||v||$  denotes the Euclidean norm of  $R^d$ . If we plot a family of  $\ln C_d(r)$  vs  $\ln(r)$  curves for different values of  $d$ , they should appear, over a limited range, as parallel lines of slope  $v$ . It turns out that  $d$  is the embedding dimension while  $v$  is the correlation exponent, related to the fractal dimension.

Figure 9 shows a family of plots described above for a laboratory experiment involving a chaotic system, in this case turbulent fluid flow. Also shown is the resultant plot of correlation exponent vs embedding dimension both for this chaotic behavior and for random "white" noise. We see that fractal dimension equals the embedding dimension for the random system but approaches the constant value of 2.8 for the chaotic system. We see, then, how this analysis clearly distinguishes between the two types of noise.<sup>14</sup>

## VI. ANALYSIS OF HgCdTe PHOTODIODE DATA

We have applied the Grassberger-Procaccia analysis to  $1/f$  noise data measured on a HgCdTe MWIR photodiode. The diode was one of an array of diodes on a chip fabricated and provided to us by Honeywell Corporation of Lexington, Mass. The chip was mounted in a low temperature Dewar (Figs. 10-11). The Dewar includes a preamplifier mounted next to the chip, and both are cooled to 80 K.

The schematic diagram of the electronics is illustrated in Figure 12. The spectrum analyzer and oscilloscope were used to verify that the noise had an ideal " $1/f$ " spectrum. We were unable to entirely eliminate 60 Hz pickup. However, by proper choice of the time interval between data points, we could insure that all of our recorded data were for frequencies below 60 Hz. Specifically, we collected 10,000 data points spaced 20 msec apart. This corresponds to a frequency range of 0.005 to 50.0 Hz. In our actual analysis, we used no more than 4000 data points, corresponding to a lower frequency of 0.0125 Hz.

The data collection network, with its A/D converter and IBM PC, could handle data of 15-bit precision. Since the  $1/f$  noise of interest was superimposed upon a much larger dc voltage, it was necessary to subtract this dc component before amplification so that we could record the noise to this precision. After this dc suppression, the noise was amplified as necessary by two PAR 113 amplifiers.

The great level of amplification required for maximum precision presented another problem. The collection of the 10,000 data points took over three minutes, and we could not maintain the sample temperature sufficiently steady over this time period. The diode resistance varies exponentially with temperature. A tiny drift in temperature during data collection would, by producing changes in the diode resistance, lead to a drift in the large dc component that we were attempting to suppress. This meant that we had to make a few adjustments to our applied suppression bias in the course of the data collection. Otherwise, the drift net dc component would saturate our amplification/collection electronics. As a result, our supposedly pure  $1/f$  noise data were contaminated by two unavoidable features, gradual drift and



sudden corrective jumps. We would need to determine if these features could cause faulty analysis by the G-P algorithm.

Meanwhile, we also needed to establish that our data were of sufficient precision and quantity for the G-P algorithm to make a proper analysis. Only with random data of infinite precision, will the G-P analysis produce a fractal dimension that increases forever with increasing embedding dimension. As soon as data are truncated to a finite precision, a deterministic element has been introduced. This will cause a lower fractal dimension. In fact, in the white noise data of Fig. 9, one can see the beginnings of a rolloff of fractal dimension at an embedding dimension of 11, no doubt caused by the limited precision of the data.

To check for the quantity of our data, the precision of our equipment, and the ability of the G-P algorithm to distinguish random from deterministic data, we used the same procedure to collect and analyze random noise as used for our  $1/f$  noise. For the random noise, we collected Johnson noise from a resistor of 16 ohms, about the same resistance as our diode sample. It should be noted that, since the random noise was collected under zero bias conditions, the data suffered no contamination with drift or jumps.

Figure 13 shows the results of the Grassberger-Procaccia analysis applied to the  $1/f$  and random noise data. The lower curve is the result obtained from analyzing 4000 data points of our  $1/f$  noise. We see that the fractal dimension does roll over and approaches a value between 9 and 10 with increasing embedding dimension. We also see that the same analysis applied to the random noise data, while not giving the ideal behavior indicated by the straight line, does give a result that differs notably from that for the  $1/f$  data. This demonstrates that the precision of our data is sufficient for the G-P analysis to detect departure from pure random behavior. To save computer expenses, only 2000 data points were used in the random noise data analysis. However, for two embedding dimensions, those of 20 and 40, we also used 4000 data points, the same as for the  $1/f$  noise data. On the graph, these are indicated by the triangles. We see how the use of more data causes the random noise analysis to approach closer to the ideal and depart farther from the behavior of the  $1/f$  noise.

This brings us to the final issue. Do the drift and jumps in the  $1/f$  noise data bring in enough of a deterministic element to account for the

resulting lowered fractal dimension? The first question addressed was that of the relative importance of drift vs jumps in the data. To determine this, we performed the G-P analysis on two subsets of the  $1/f$  data, each of which contained 1350 data points. The first subset had strong drift but no jumps, while the second subset had a number of jumps and practically no drift. For the embedding dimension of 30, the fractal dimensions were 9.902 and 8.168, respectively. We also analyzed a subset of 2000 data points which contained the drift data of the first subset plus a few jumps among the additional data points. The fractal dimension for this subset came to 9.247. It appears from these comparisons that jumps do lower the fractal dimension and do so far more effectively than does drift.

Given that jumps were present in the  $1/f$  data and absent in the random data, and given that jumps lower the value of the fractal dimension as determined by the G-P analysis, we must investigate whether the disparity between the two types of data could be the result of these jumps. To do this we performed the G-P analysis on the following two sets of data. The first consisted of 2000 points of  $1/f$  data which contained four jumps but no drift. The second was 2000 points of random noise data in which we had artificially added four jumps of the same relative magnitude and spacing as in the first set. The resulting fractal dimensions were 7.928 and 13.8, respectively. We conclude that, although the jumps have depressed the fractal dimension of the random noise data, they have not done so nearly enough to account for the disparity between the fractal dimensions calculated for the two types of data.

We believe, on the basis of this analysis, that the true explanation of  $1/f$  noise can be found only in the mathematical discipline of chaos theory, not in the exclusively random mechanisms that have been previously investigated.

## VII. CHAOTIC MODELING OF 1/f NOISE

Establishing the chaotic nature of 1/f noise does not, in itself, answer the question of its origin. Rather, it redirects the direction of theoretical investigation. It points us away from random processes towards deterministic ones. We have made an initial attempt towards constructing a chaotic theory model of 1/f noise. Our model makes use of what is known about 1/f noise from both general investigations and investigations specific to HgCdTe. It also includes criteria for chaotic behavior known from chaos theory.

From chaos theory, we know that the equations must possess both nonlinearity and dissipation. From general 1/f noise data, it appears that a geometrical constraint plays a vital role and that mobility, in particular, is strongly affected. Finally, from HgCdTe 1/f noise data, we conclude that generation-recombination processes drive the 1/f noise.

To include all of this in our model, we begin with the continuity-diffusion equation applied to the carriers.

$$\rho_t + (\mu E \rho)_x - D \rho_{xx} = -4\pi\tau\rho \quad (1)$$

This links the carrier concentration,  $\rho$ , to the mobility,  $\mu$ . Also included are the electric field,  $E$ , the diffusion coefficient,  $D$ , and the generation-recombination lifetime,  $\tau$ . To complete the nonlinear coupling between the carrier concentration and the mobility, as well as to explicitly include dissipation, we note that the mobility is a function of temperature to the 3/2 power; the local temperature, in turn, depends upon the local resistivity via Joule heating, and that resistivity depends upon the mobility and carrier concentration via

$$\text{resistivity} = (q\mu\rho)^{-1} \quad (2)$$

We further use the geometrical arrangement of Fig. 14. This has two normal mobility regions separated by a low mobility barrier. This barrier corresponds to the depletion region of a p-n junction such as that which exists in a HgCdTe photodiode. We take  $\tau$  as non-zero only in this barrier region, as we expect to be the case in reality.

All of these features are factored into a computer program that we have written for an IBM PC. The program uses the values of  $\rho$  and  $\mu$  as a function of position at one time and then calculates new values for the succeeding moment. The computer code is provided in the appendix.

Figure 15, which shows the mobility vs time, is a typical output of such a calculation. Also in Fig. 15, we provide a log-log plot of the Fourier analysis of this output. The straight line which overlays the calculated data points corresponds to

$$y \text{ axis} = \text{frequency}^{-1}$$

indicating a  $1/f$  type spectrum over most of the range.

### VIII. SUMMARY

We have obtained strong evidence that  $1/f$  noise is chaotic, rather than random, in origin. We have also begun to construct a model of  $1/f$  noise in HgCdTe photodiodes based upon chaos theory and the results of experimental investigations. This simulation has produced noise with a  $1/f$ -like spectrum. However, considerable development is required. For example, the model gives a power spectral density dependence of frequency<sup>-2</sup> rather than the sought for frequency<sup>-1</sup> and includes a random driver, specifically, the generation-recombination mechanism.

We believe that the latter difficulty can be readily eliminated; the g-r process can be duplicated using deterministic, rather than the random processes now employed. With that change, it may be found that the power spectral density converts to the desired frequency<sup>-1</sup> dependence.

## REFERENCES

1. K. M. van Vliet, "Noise in Semiconductors and Photoconductors." Proceedings of the IRE 46, 1004 (1958).
2. P. H. Handel, "Quantum Approach to 1/f Noise." Phys. Rev. A 22, 745 (1980).
3. F. N. Hooge, T. G. M. Kleinpenning, and L. K. J. Vandamme, "Experimental Studies on 1/f Noise." Reports on Progress in Physics 44, 479 (1981).
4. M. B. Weissman, "Survey of Recent 1/f Noise Theories." Noise in Physical Systems. Proceedings of the 6th International Conference on Noise in Physical Systems N.B.S. Special Publication no. 614, 133 (1981).
5. P. Dutta and P. M. Horn, "Low-Frequency Fluctuations in Solids: 1/f Noise." Reviews of Modern Physics 53, 497 (1981).
6. W. A. Radford and C. E. Jones, "Influence of Surface Tunnel Currents on 1/f Noise in HgCdTe Photodiodes." J. Vac. Sci. Technol. A 3 (1985).
7. H. K. Chung, M. A. Rosenberg, and P. H. Zimmerman, "Origin of 1/f Noise Observed in MW (Hg,Cd)Te Variable Area Photodiode Arrays." J. Vac. Sci. Technol. A 3, 189 (1985).
8. J. Bajaj, G. M. Williams, N. H. Sheng, M. Hinnrichs, D. T. Cheung, J. P. Rode, and W. E. Tennant, "Excess (1/f) Noise in  $\text{Hg}_{0.7}\text{Cd}_{0.3}\text{Te}$  p-n Junctions." J. Vac. Sci. Technol. A 3, 192 (1985).
9. F. N. Hooge, "Experimental Facts of 1/f Noise." Proceedings of the Symposium on 1/f Fluctuations, Tokyo, Japan, 11-13 July 1977, Sponsored by the Institute of Electrical Engineers of Japan.
10. T. G. M. Kleinpenning, "On 1/f Noise in Reverse-Biased P-N Junction Diodes." Noise in Physical Systems and 1/f Noise Eds. M. Savelli, G. Lecoy, and J-P. Nougier: Elsevier Science Publishers, 1983.
11. J.-P. Eckmann, "Roads to Turbulence in Dissipative Dynamical Systems." Reviews of Modern Physics 53, 643 (1981).
12. D. Ruelle and F. Takens, "On the Nature of Turbulence." Commun. Math. Phys. 20 (1971), 167.
13. P. Grassberger and I. Procaccia, "Estimation of the Kolmogorov Entropy from a Chaotic Signal." Physical Review A 28, 2591 (1983).
14. J. P. Eckmann and D. Ruelle, "Ergodic Theory of Chaos and Strange Attractors." Rev. Mod. Phys. 20, 167 (1971).

FIGURES

# Typical Time Series and PSD for 1/f Noise

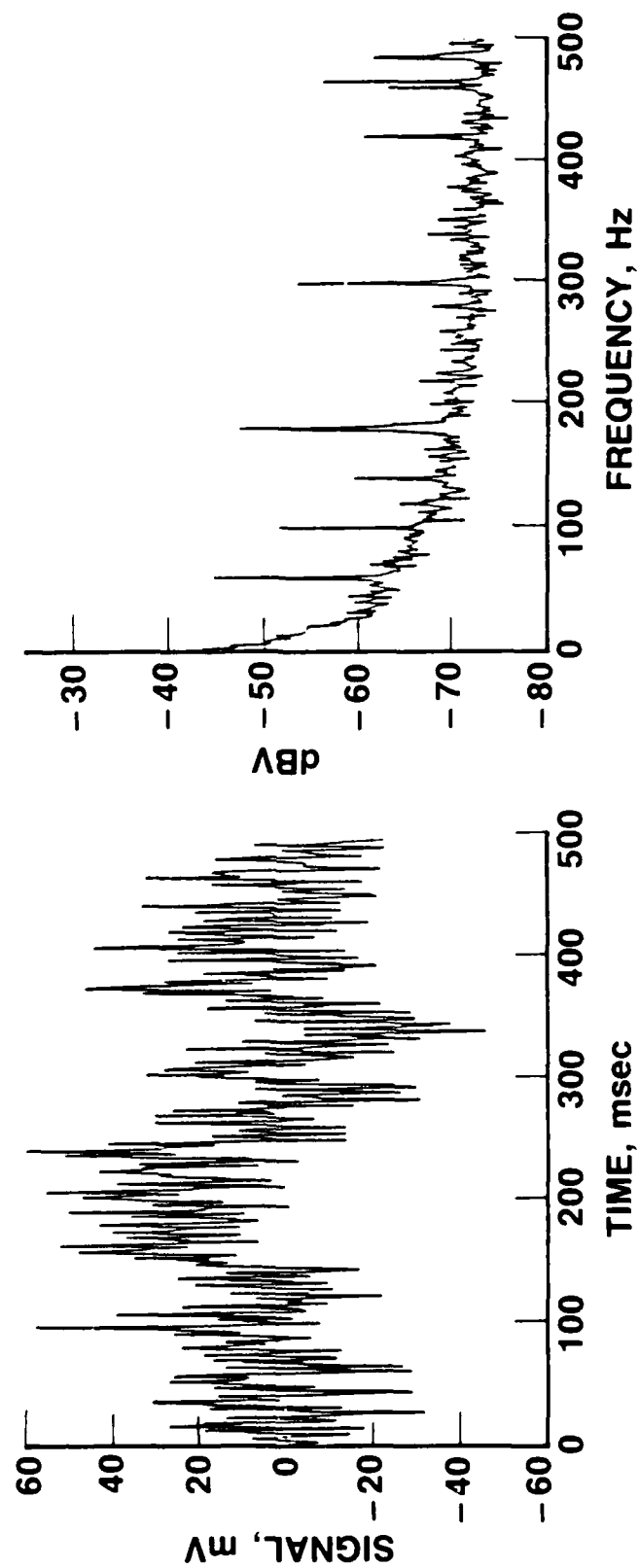
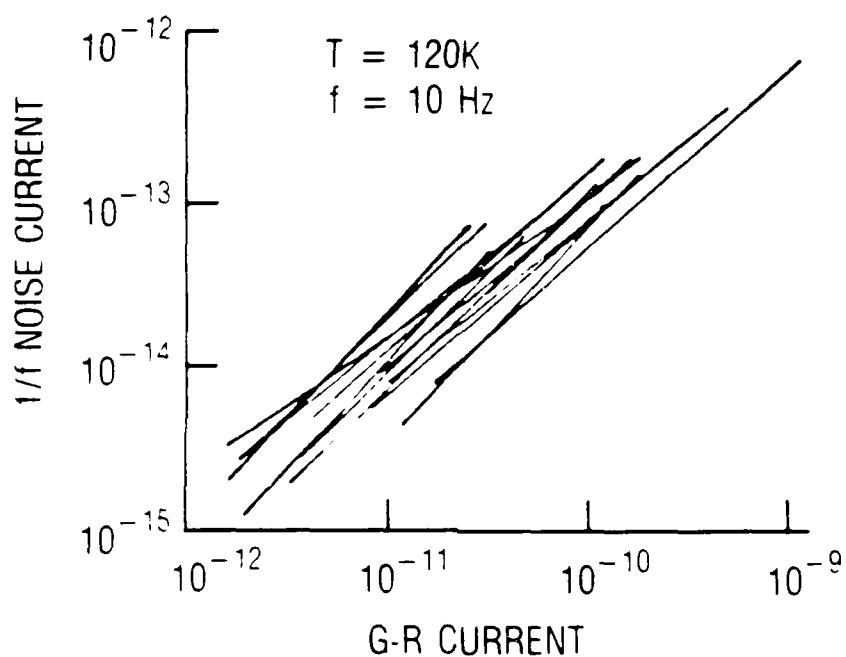


Fig. 1



## Correlation Between 1/f Noise and G-R Current



PLOT OF 1/f NOISE CURRENT AT 10Hz vs G-R CURRENT  
FOR 14 VARIABLE AREA  $\text{Hg}_{0.7}\text{Cd}_{0.3}\text{Te}$  PHOTODIODES

Fig. 2

# 1/f Noise VS Total Number of Carriers

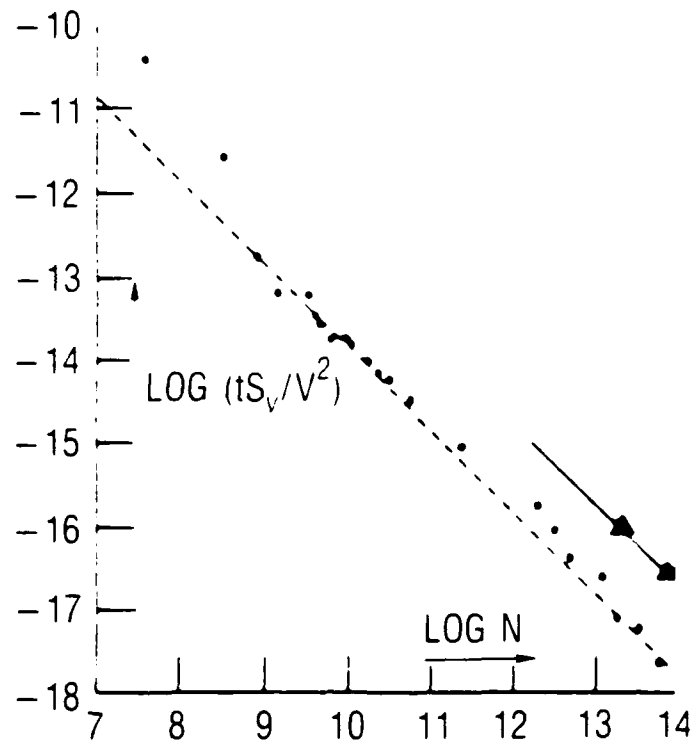


Fig. 3

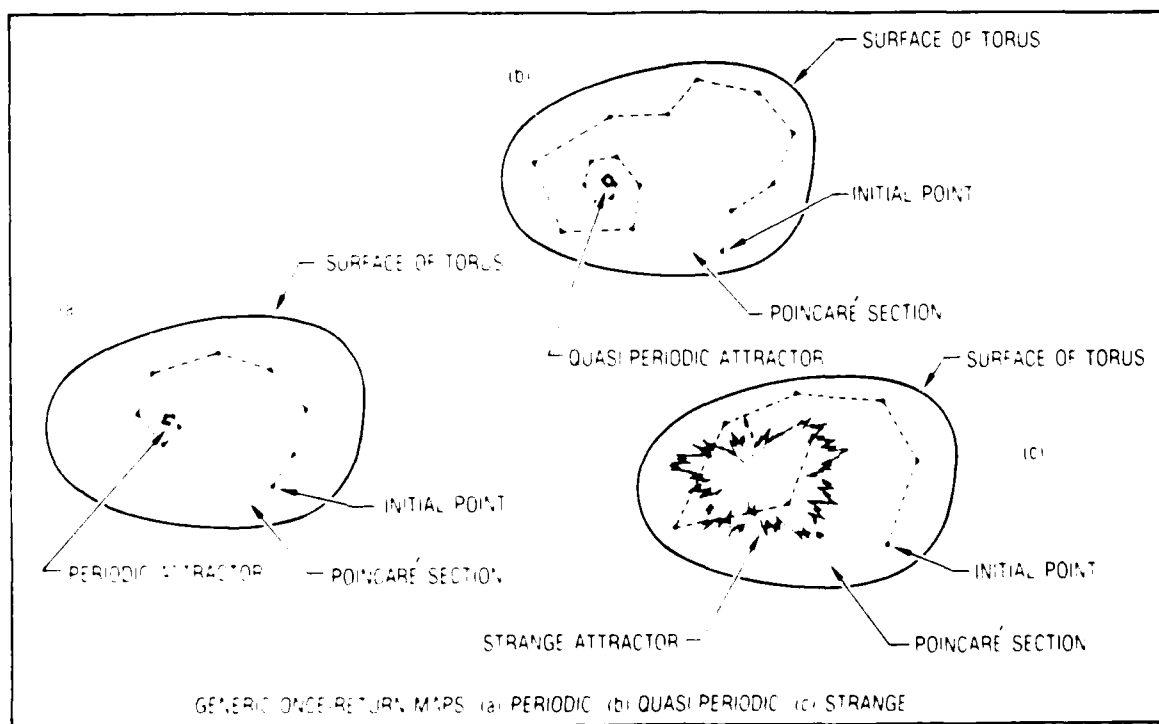
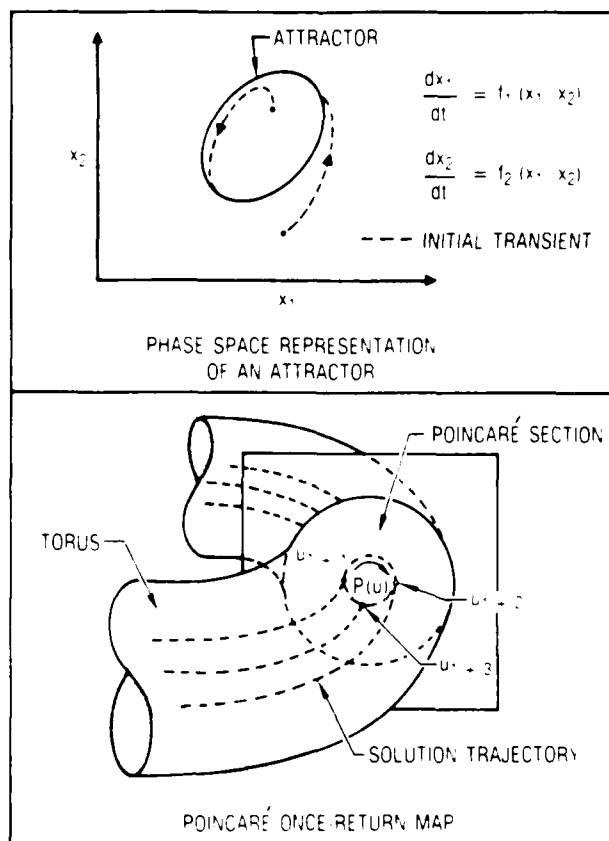


Fig. 4

# The Henon Attractor

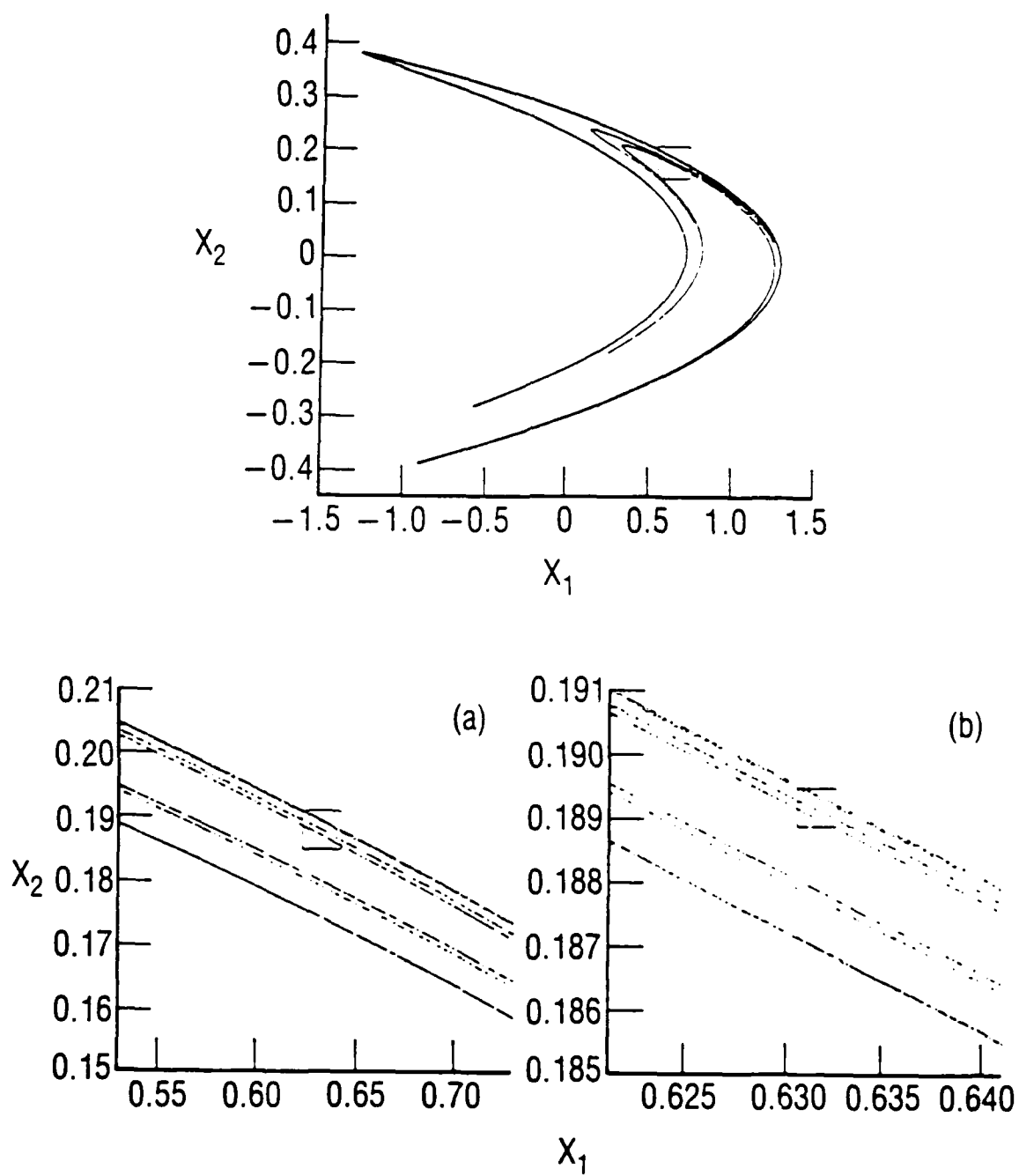


Fig. 5

## Plot of $X_2$ Parameter Against Time

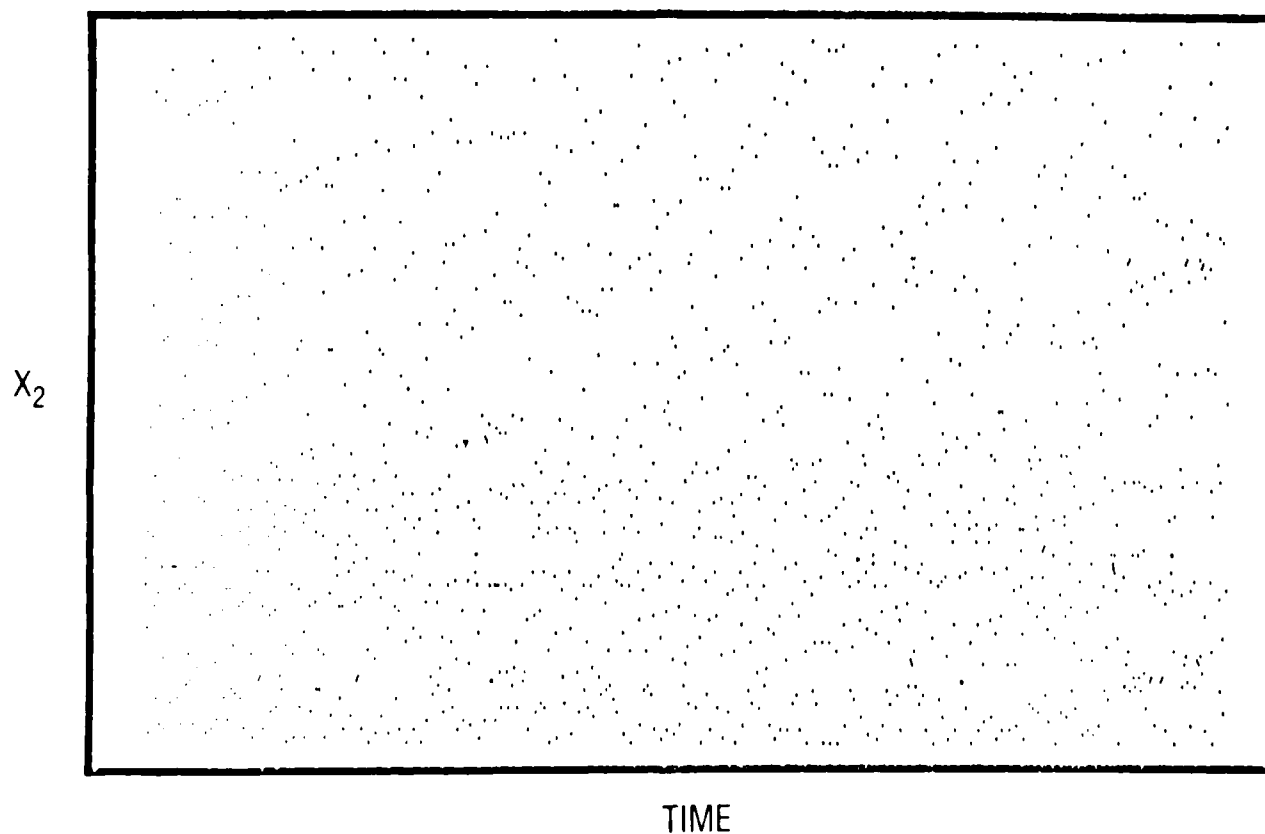
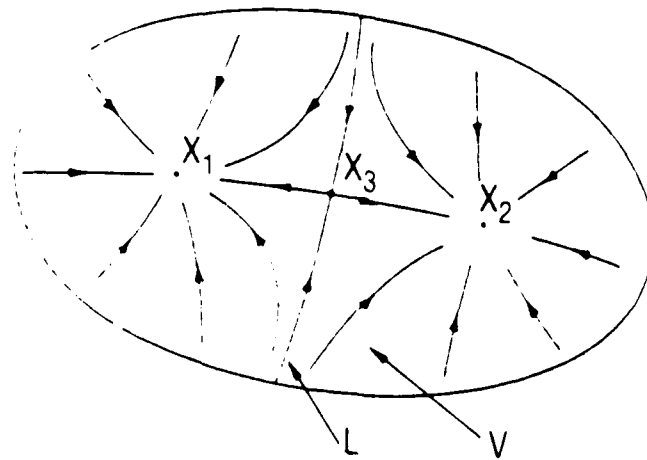


Fig. 6

## Example of the Bifurcation of Attractors



PHASE PORTRAIT ILLUSTRATING TWO STABLE ( $X_1$ ,  $X_2$ ) AND ONE UNSTABLE ( $X_3$ ) FIXED POINT



PHASE PORTRAITS ILLUSTRATING HOPF BIFURCATION

Fig. 7

# Emergence of a $1/f$ -Like Spectrum Upon Bifurcations of an Attractor

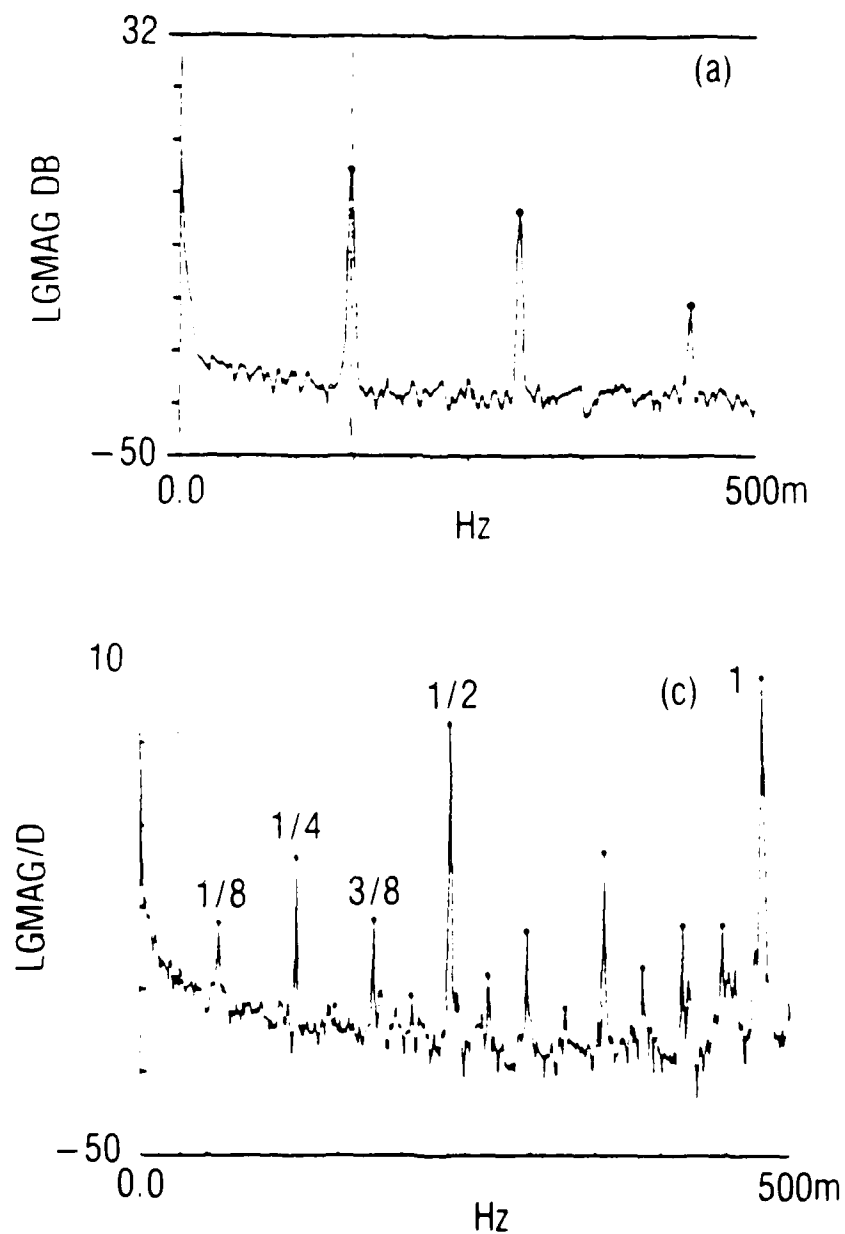


Fig. 8

# Grassberger-Procaccia Exponent for Turbulent Flow

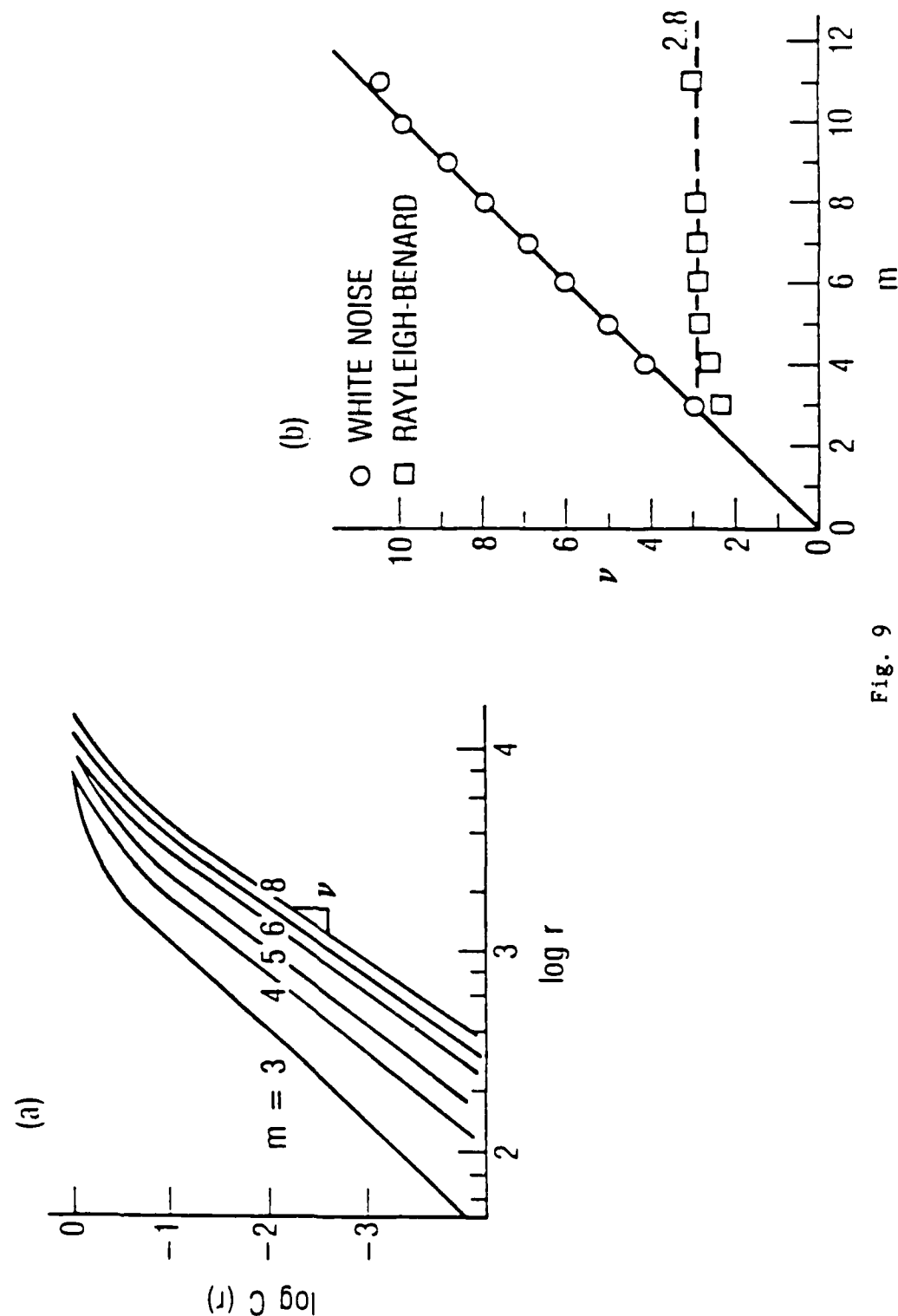


Fig. 9



# Low Temperature Dewar (Down to 4.2K) for 1/f Noise Measurements

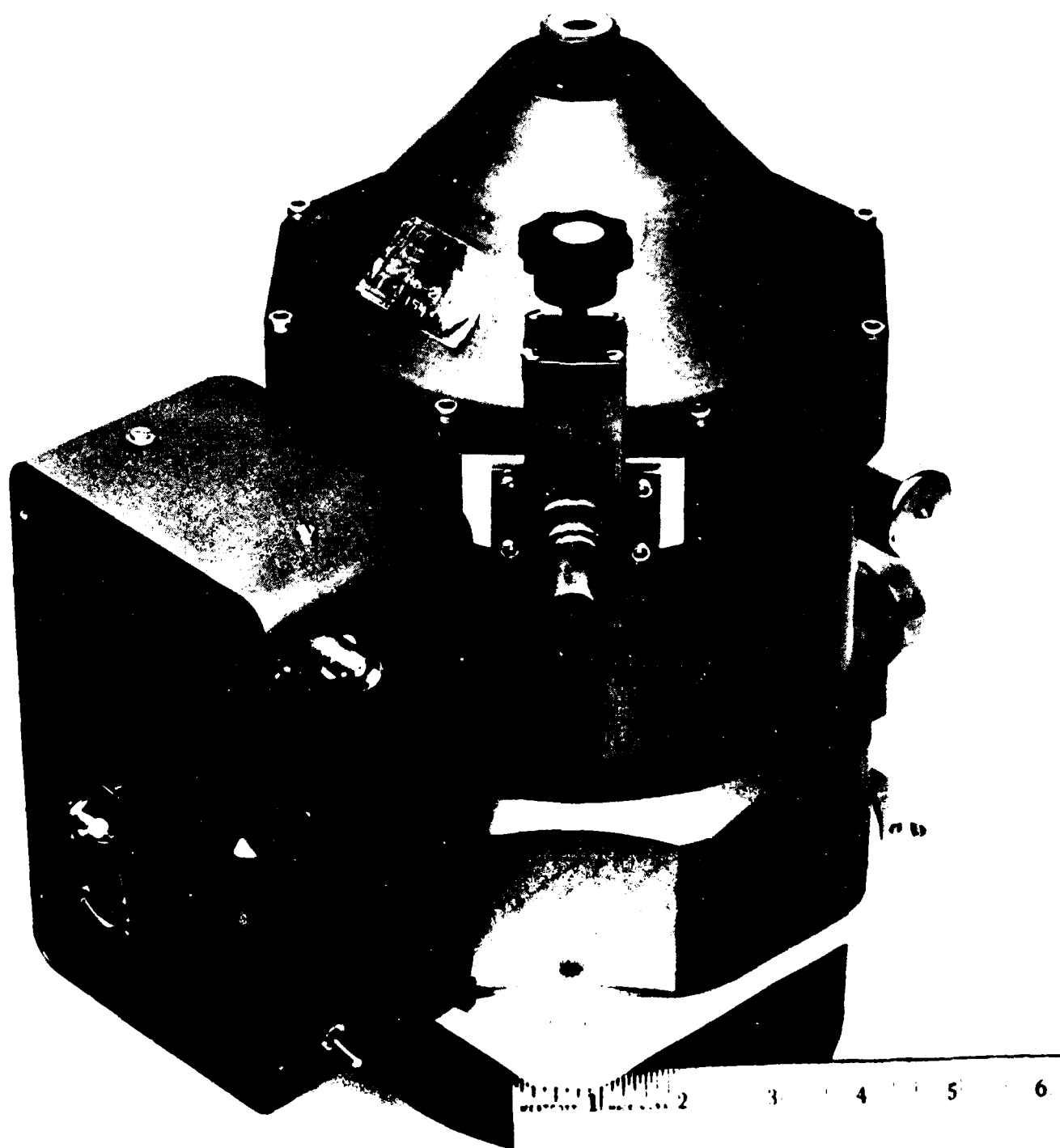


Fig. 10

# Mounting Arrangement for Photodiode Array and Low Temperature Amplifier

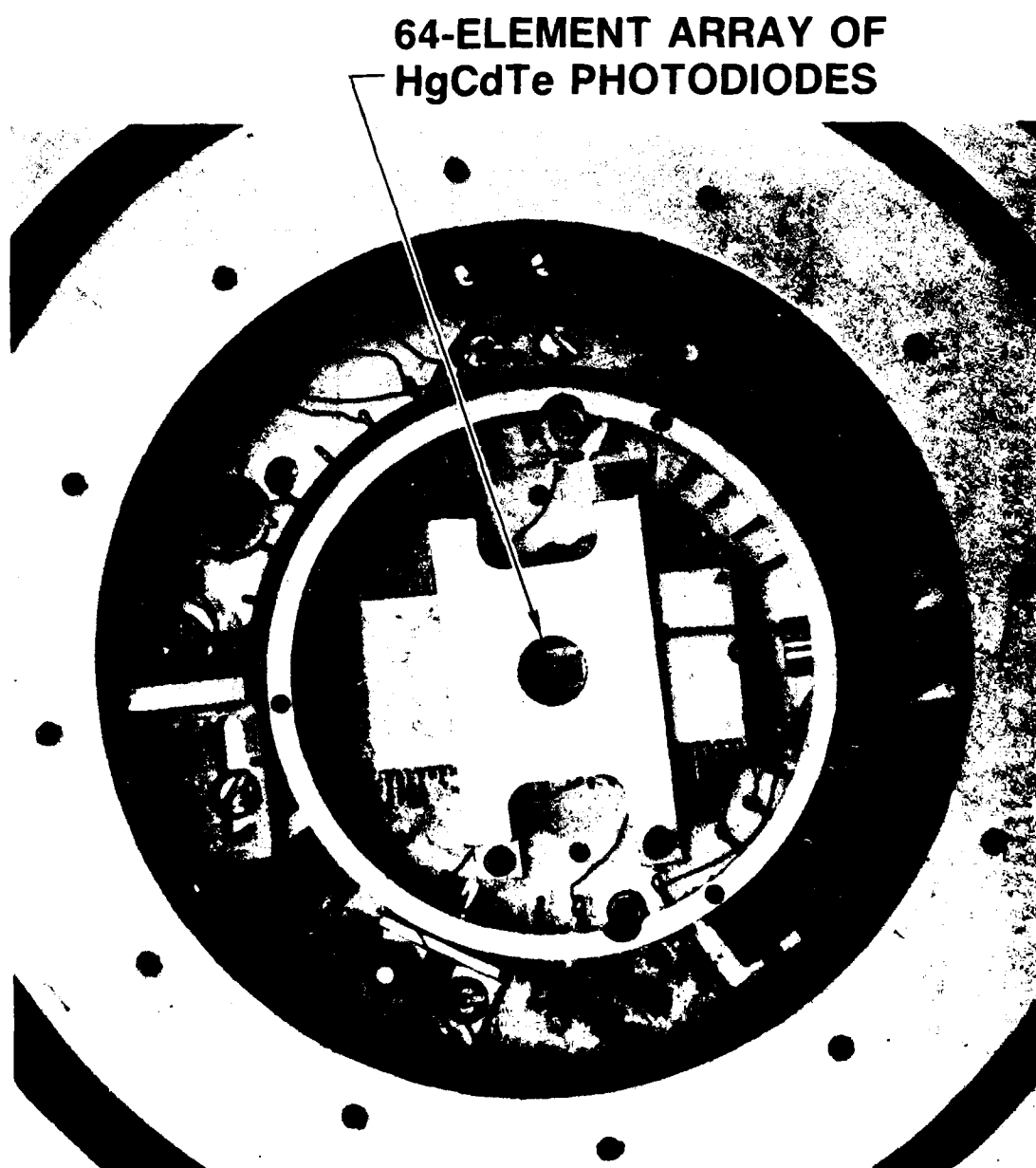
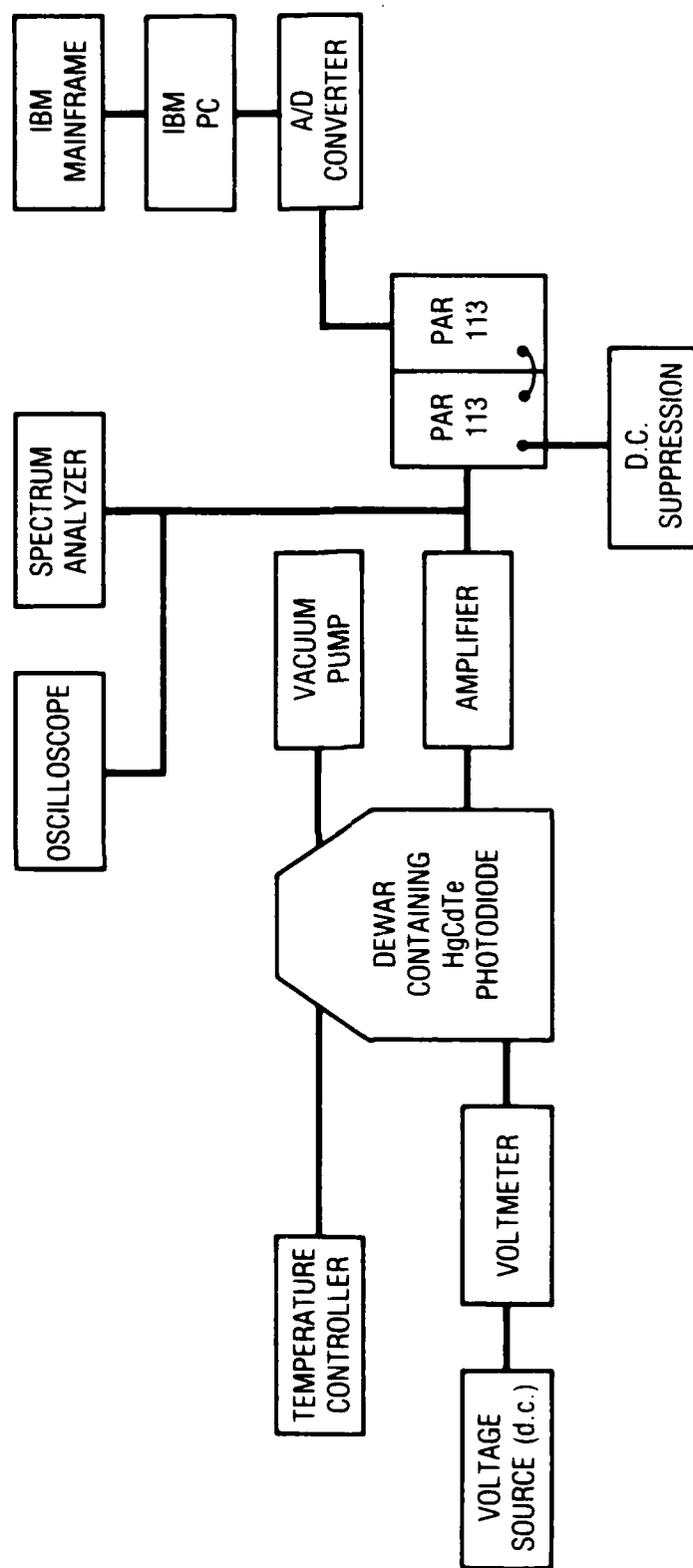


Fig. 11

# Laboratory Experiments on HgCdTe Semiconductors



SCHEMATIC OF APPARATUS

Fig. 12

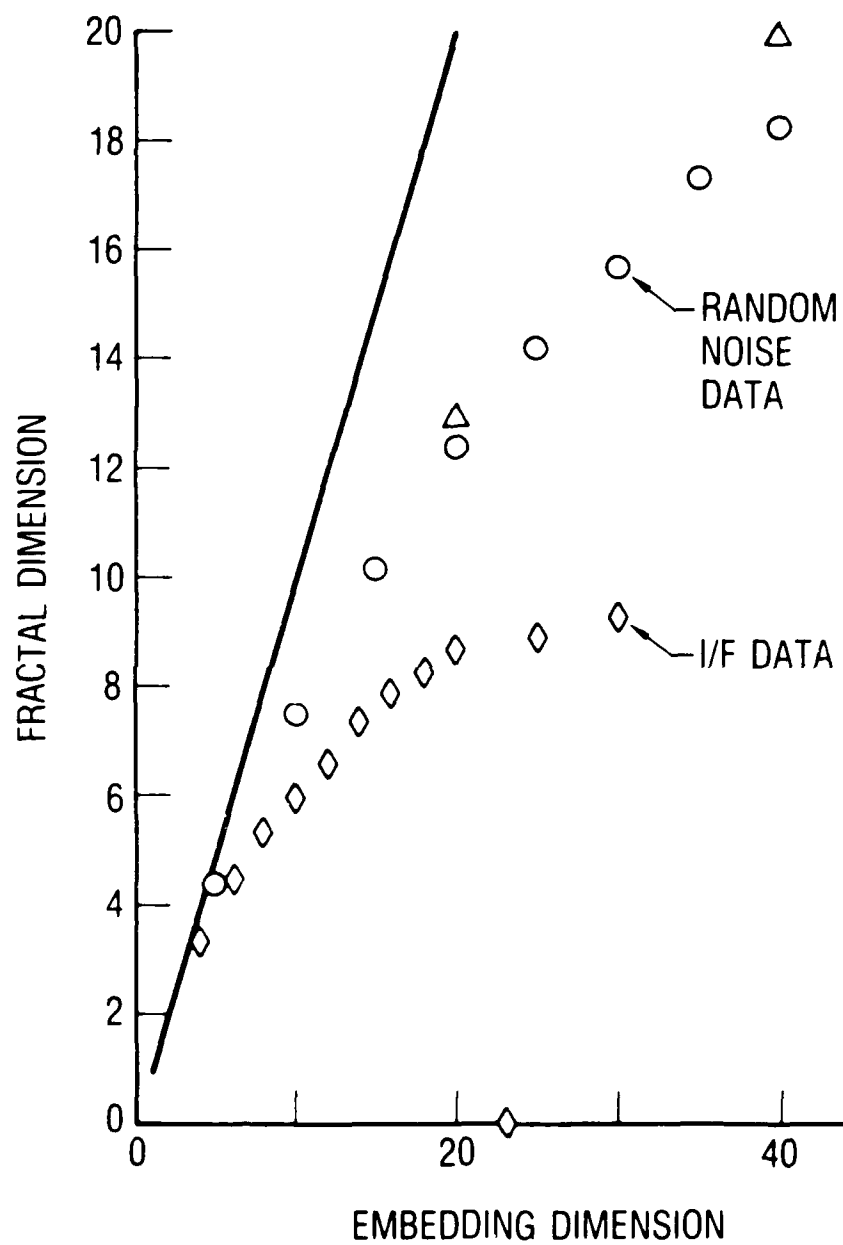


Fig. 13

## GEOMETRY OF MODEL

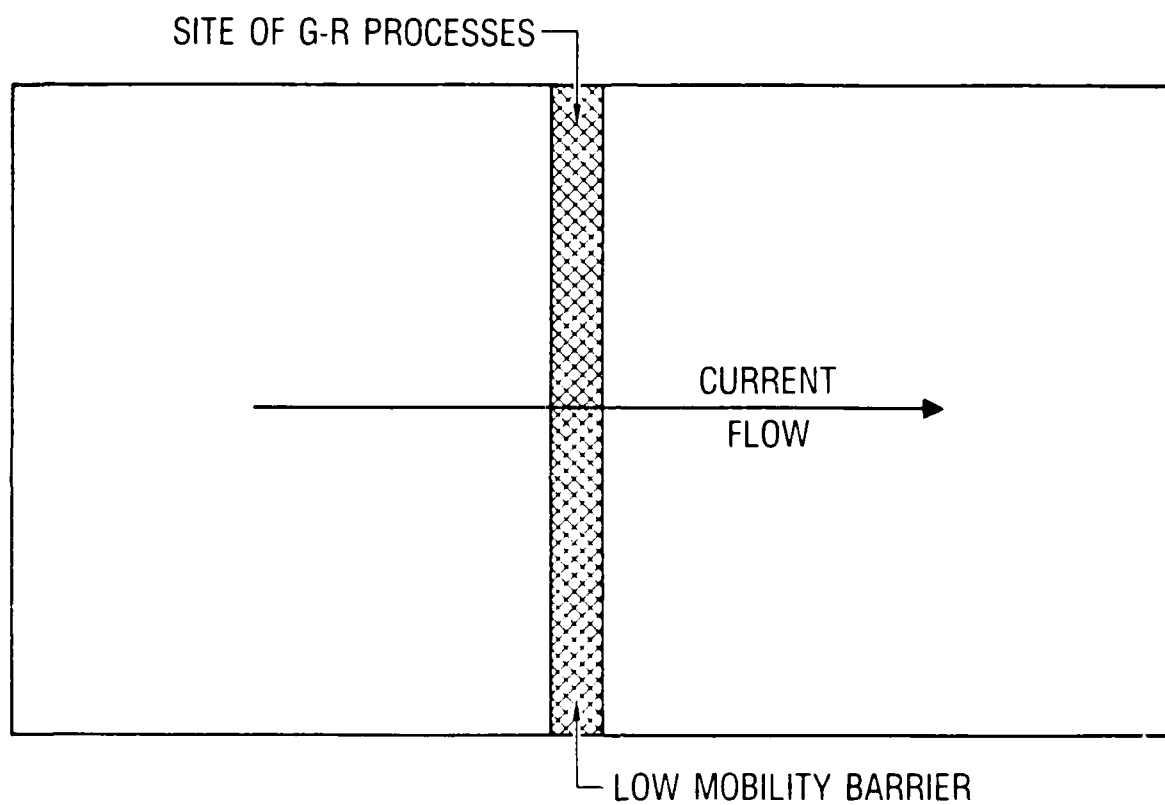


Fig. 14

# Model Predictions

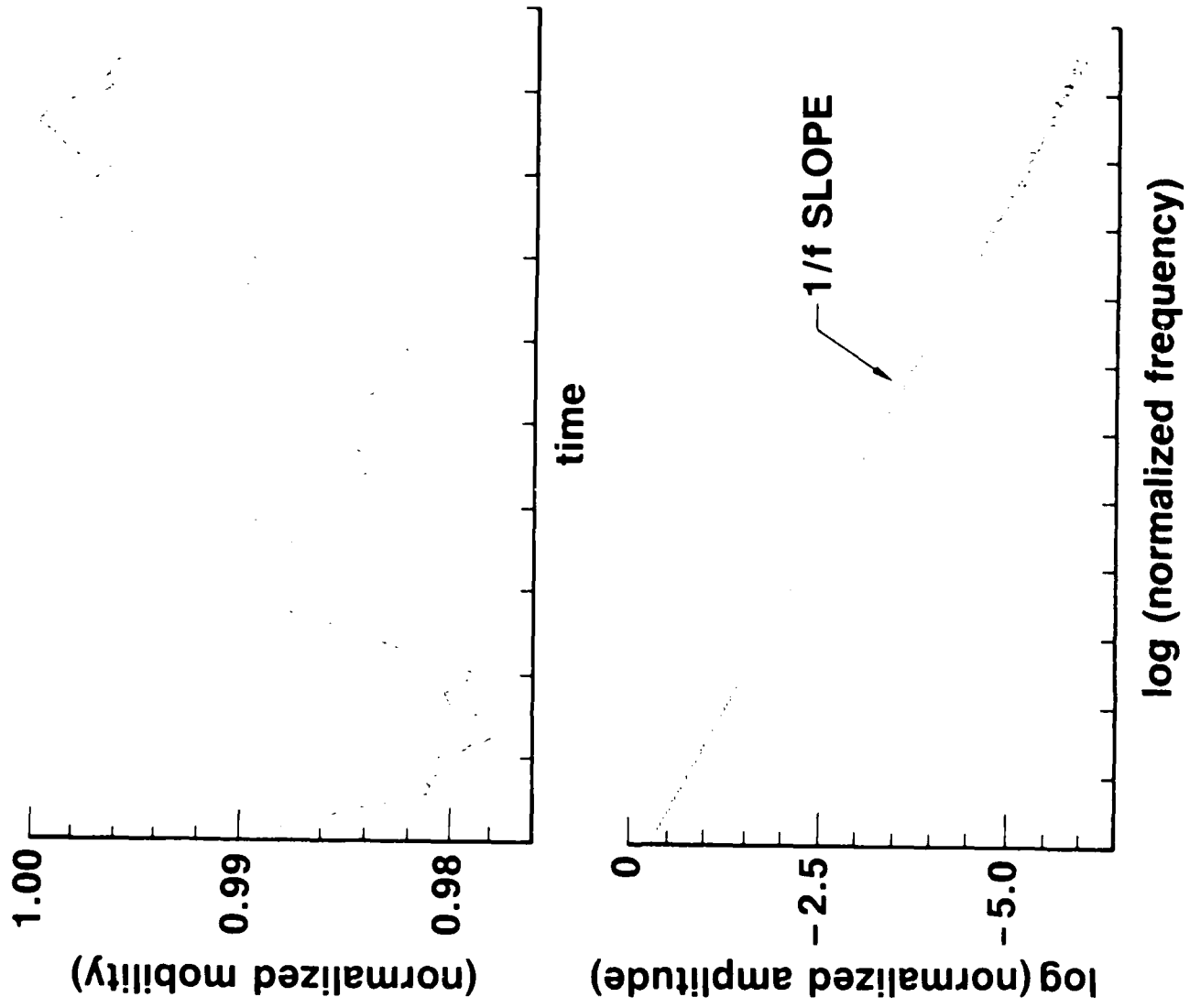


Fig. 15

## APPENDIX: COMPUTER CODE FOR THE $1/f$ NOISE MODEL

In this appendix, we provide the calculation segment of the computer code of our  $1/f$  noise model. The programming language is Pascal. The temperature is designated by "t" the electric field by "e", and the departure from the equilibrium temperature, caused by local Joule heating, by "dtemp". "i" and "j", the coordinates of our two-dimensional lattice, run from 1 to m, with m usually taken as 5. The central strip defined by  $i=3$  has lower mobility than the surrounding lattice points and represents the depletion region of the p-n junction. The index "k" designates the time. The output coordinate is the quantity "dat", representing the mobility at the central lattice point (3,3).

```

dx := 1 E - 6;
dt := 1 E - 12;
For i := 1 To m Do
Begin
For j := To m Do
Begin
dr[i,j] := 0.0;
mu[i,j] := 1.0;
tau[i,j] := 0.0;
rho[i,j] := 1/Sqr(m);
If (i = 3) Then mu[i,j] := 0.001;
End;
End;
Begin;
For i := 2 to m-1 Do
Begin
For j := 2 to m-1 Do
Begin
dtemp := 0.1 * (mu[i,j]*rho[i,j] * Sqr(m) - 1,0);
d := (8.625E-5) * Exp((3/2) * Ln(1+dtemp))
      * mu[i,j] * t * dt/(dx*dx);
dr[i,j] := d * (rho[i,j-1] + rho[i,j+1] - 2 * rho[i,j]);
dr[i,j] := d * (rho[i-1,j] + rho[i+1,j] - 2 * rho[i,j] + dr[i,j]);
dr[i,j] := -(rho[i,j] * Exp((3/2) * Ln(1+dtemp))
      * mu[i,j] - rho[i-1,j] * Exp((3/2) * Ln(1+dtemp))
      * mu[i-1,j]) * e * dt/dx
      + dr[i,j];
dr[i,j] := - (rho[i,j] * Exp((3/2) * Kb(1+dtemp))
      * mu[i,j] - rho[i,j-1] * Exp((3/2) * Ln(1+dtemp))
      * mu[i,j-1]) * e*dt/dx
      + dr[i,j];
If (i = 3) Then tau[i,j] := (2E8) * (random - 0.5);
dr[i,j] := 4 * 3.1416 * tau[i,j] * dt + dr[i,j];
End;
End;
For i := 1 to m Do
Begin
For j := 1 to m Do
Begin
rho[i,j] := rho[i,j] + dr[i,j];
End;
End;
End;
dat := Exp((3/2) + Ln(1+dtemp)) * mu[3,3];
End:

```